

# DEVELOPING A METHODOLOGY FOR IMPROVING THE EFFICIENCY OF THE COMPACTION OF A BASE COURSE WITH A SINGLE-DRUM VIBRATORY ROLLER

**Kalin Radlov**✉

*Department of Construction Technology and Mechanization<sup>1</sup>*  
kradlov@abv.bg

**Lachezar Lazov**

*Department of Manufacturing Automatization<sup>2</sup>*

**Andrey Totsev**

*Department of Geotechnics<sup>1</sup>*

**Lachezar Hristchev**

*Department of Construction Technology and Mechanization<sup>1</sup>*

<sup>1</sup>*University of Architecture, Civil Engineering and Geodesy – Sofia*  
*1 Hristo Smirnensky str., Sofia, Bulgaria, 1046*

<sup>2</sup>*Technical University – Sofia*  
*8 Kliment Ohridsky str., Sofia, Bulgaria, 1000*

✉ Corresponding author

---

## Abstract

The object of the study is a single-drum vibratory roller, which is widely used in construction technology. It presents a theoretical investigation on improving compaction efficiency, focusing on the compaction process of a base course for foundations with a specified model of a single-drum vibratory roller, including various soil types. In the present study is considered a methodology for the optimal combination between the technical data of the roller (e.g.: own weight of the roller, excitation frequency, etc.) and the mechanical characteristics of the compacted material (e.g.: material density, elasticity modulus, etc.). The current analysis is based on a mathematical model of a vibratory roller with three degrees of freedom, for which differential equations of dynamic motion are obtained. The equations of motion are solved for an exemplary model of vibratory roller, using five different types of compacted material, as well as three possible input excitation frequencies. For each of the cases is calculated the maximum amplitude of vibratory compaction motion which is obtained under the roller steel drum (the so called: "compaction amplitude"), on which the compaction efficiency is most dependent, i.e. as high the compaction amplitude is, as better the compaction efficiency is. For the exemplary vibratory roller model used in this study, the analysis shows that at an excitation frequency of 25 Hz, compaction is 1.19 times more effective (corresponding to a 19% higher compaction amplitude) when applied to granular soils with small particles (up to 0.5 cm) compared to granular soils with large particles (up to 10 cm). The presented methodology can be useful for practicing engineers when performing an optimal selection of a vibratory roller model for assigned compaction work, helping them to improve the efficiency and productivity of the performed compaction work at the building site.

**Keywords:** vibratory roller, efficiency, dynamic motion, base course, soil type, compaction amplitude.

DOI: 10.21303/2461-4262.2025.003925

---

## 1. Introduction

In recent years, there has been a tendency in construction to use more efficient compaction equipment for the preparation of the ground surface under building and road foundation bases. The compaction efficiency has been recognized by many structural engineers as one of the most important factors affecting road base and building foundation performance. The improvement of a vibratory roller efficiency depends on machine design considerations (including: improved technical characteristics of the selected construction equipment) on one hand, as well as on some technological considerations on the other hand (including: optimal combination of vibratory roller model and compacted soil type), which could help to improve the efficiency of compaction work at the building site.

There are many studies discussing the working process of rollers which are concerned with different problems of their usage, as for examples: papers [1–3] are focused on the improvements of an anti-vibration system under the operator's seat for better ride comfort, through analysis of different cab mounts and control of vibrations in roller suspension system. Paper [4] analyses the productivity of the roller under various working conditions, while papers [5, 6] deals with roller design parameters for compaction of agricultural soils. There is also another existing study [7], which is focused on investigation of static and quasi-static loads of an asphalt roller for several load cases, which are in consideration during the design to identify high forces and heavy bending moments in machine structure. Paper [8] deals with the expected advantages and benefits by increasing the number of drums on the tandem roller from 2 to 3, while paper [9] deals with the state-of-the-art of the quality control and quality assurance methods for earthwork compaction in roads, railways, airports, dams, and embankment construction, whereby various problems existing have been partially resolved to achieve more effective compaction quality control and construction efficiency improvement. Another paper [10] deals with innovative ideas, as the expected benefits from the use of a vibratory pneumatic type roller, while in the paper [11] are performed analyses on the horizontal oscillating vibrations of a vibratory roller.

Many of the existing studies are devoted to roller control systems and compaction monitoring technologies analysis, as for example: paper [12] deals with different compaction technologies and considers induced cracks at the asphalt compacted layer, which allows moisture to permeate into the pavement, accelerating stripping, fatigue, and deterioration, while in the paper [13] it is proposed an automatic navigation algorithm of an articulated drum roller, through which can be improved the work efficiency and operation cost. Paper [14] represents different possible measurement technologies, which can be used by different models of drum rollers, while paper [15] deals with design of a detection system for drum roller, significantly improving defect image contrast, which could enhance the roller compaction performance in real-world scenarios. These studies, which are focused on improving the working process and compaction efficiency of vibratory rollers are of particular interest to structural engineering. For example, paper [16] examines the effect of the excitation frequency of the vibratory machine on the compaction process of non-cohesive soils (sandy soils, gravel, etc.). Paper [17] is analyzed a single-degree of freedom dynamic model of a vibratory roller to consider the vertical drum motion, while taking into account the variable contact width between drum and soil, while in another research paper [18] it is used a practical single-degree-of-freedom dynamic model to analyze the characteristics of the vibratory roller drum and to study the nonlinear dynamic behavior of the roller on different elastic subgrades, through which the drum "bouncing" motion can be avoided. Further, papers [19, 20] analyze the dynamic behavior of the vibratory roller-compacted soil system by using mathematical models with two degrees of freedom, without analyzing the effect of the compacted material type on the vibratory amplitude.

The absence of an overall analytical model of the "vibratory roller – compacted material" system, as well as a methodology for determining the most appropriate combination between a type of vibratory roller (including excitation frequency, roller weight, etc.) and the mechanical characteristics of the compacted material (including material density, elasticity modulus, etc.), can be considered as a gap in the existing research literature.

The objective of the present study is to propose such an analytical model and methodology, that can help practicing engineers to improve the efficiency and productivity of compaction work performed at construction sites.

The tasks of the present research are as follows:

1. To develop an overall mathematical model with three degrees of freedom for the "vibratory roller – compacted material" system, through which the vibration amplitude (i.e. amplitude of compaction) of the roller's steel drum can be determined.
2. To present an analytical methodology aimed at improving the efficiency of compaction work with single-drum vibratory rollers at construction sites, focusing on technological considerations – specifically, on identifying the most appropriate combination between the vibratory roller parameters (including excitation frequency, roller weight, etc.) and the mechanical characteristics of the compacted material (including material density, elasticity modulus).

3. To provide an example, which demonstrates the application of the proposed methodology using a model of a single-drum vibratory roller with three possible excitation frequencies and five different types of compacted materials.

## 2. Materials and methods

The object of the study is a single-drum vibratory roller, a common view of which is presented in Fig. 1.

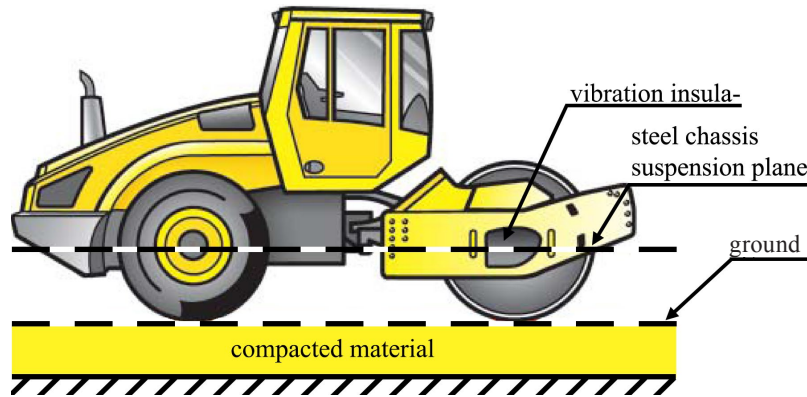


Fig. 1. Common view of a single-drum vibratory roller

The central hypothesis of this study is that the vibration amplitude of the roller's steel drum (i.e. the compaction amplitude) represents the most reliable indicator of roller compaction efficiency, particularly during the compaction of non-cohesive soils. Specifically, greater compaction amplitudes of the roller's steel drum are assumed to correspond to higher compaction efficiency.

During the modelling process, the following simplifications for a single-drum vibratory roller (Fig. 1) were applied: it was assumed that the two chassis suspension points located at both ends of the roller lie in the same horizontal plane, and that the chassis rotation angle is sufficiently small such that:  $\sin \theta \approx \tan \theta \approx \theta$ . Furthermore, the horizontal vibration amplitude of the chassis was assumed to be negligible low, compared to its vertical vibration amplitudes, therefore only the vertical vibration transfer was considered. It was also assumed that: the stiffness of the roller's steel chassis and steel drum approximates that of an ideal rigid body; the self-weight of the roller is evenly distributed between its two rear pneumatic tires; it is assumed linear dynamic behavior of soil upper layer and constant stiffness of the compacted material.

It is assumed, that the total value of the exciting vibrational force in the front steel drum of roller  $F_{DEB}$  in  $N$  is caused by two unbalanced rotating shafts in opposite directions. That force can be calculated according to the equation of dynamic force  $F$  in  $N$ , which is given in the Eurocode standards EN 1991-3 [21], namely:

$$F = m_1 e_1 \omega_1^2, \quad (1)$$

$$F_{DEB} = 2m_1 e_1 \omega_1^2 \sin(\omega_1 t), \quad (2)$$

where  $e_1$  – the eccentricity of the two unbalanced rotating shafts inside the front steel drum in  $m$ ;  $m_1$  – own mass of the two unbalanced rotating shafts in  $kg$ ;  $\omega_1$  – angular velocity (rotational speed) of the two unbalanced rotating shafts in  $rad/sec$ .

The differential equations of the dynamic motion under harmonic excitation are obtained by using the energy method with Lagrange's equations [22] i.e.:

$$\frac{d}{dt} \left( \frac{\partial E_K}{\partial \dot{x}_1} \right) - \frac{\partial E_K}{\partial x_1} + \frac{\partial R}{\partial x_1} + \frac{\partial E_P}{\partial x_1} = Q_{X1}, \quad (3)$$

$$\frac{d}{dt} \left( \frac{\partial E_K}{\partial \dot{x}_2} \right) - \frac{\partial E_K}{\partial x_2} + \frac{\partial R}{\partial \dot{x}_2} + \frac{\partial E_P}{\partial x_2} = Q_{X2}, \quad (4)$$

$$\frac{d}{dt} \left( \frac{\partial E_K}{\partial \dot{x}_3} \right) - \frac{\partial E_K}{\partial x_3} + \frac{\partial R}{\partial \dot{x}_3} + \frac{\partial E_P}{\partial x_3} = Q_{X3}, \quad (5)$$

where  $E_K$  – the kinetic energy of the system as a function of generalized coordinates and generalised velocities in J;  $E_P$  – the potential energy of the system as a function of generalized coordinates in J;  $R$  – the dissipation function, based on generalized velocities in J/s;  $\dot{x}_i$  – generalized speeds in m/s;  $x_i$  – generalized coordinates of the dynamic system in m ( $i = 1, 2$  and  $3$ );  $Q_{Xi}$  – corresponding external applied loading in each generalized coordinate in N.

The differential equations of dynamic motion (3)–(5) are solved by using the software product MATLAB.

For the present research article, the values of the damping coefficients  $b$  in N.s/m are calculated by the following equation

$$b = 2\zeta\sqrt{mc}, \quad (6)$$

where  $\zeta$  – the damping ratio, which for the present analysis is assumed to be as follows:  $\zeta = 63\%$  (for the vibration insulator and rear pneumatic tires),  $\zeta = 5\%$  (for the steel frame of the chassis) and  $\zeta = 80\%$  (for the compacted material).

For the purposes of the present study it is accepted to calculate the approximate value of the stiffness coefficient for the compacted material  $c_3$  in N/m using the following equation

$$c_3 = \frac{E_M S_{CP}}{d}, \quad (7)$$

where  $E_M$  – the elasticity modulus of the compacted material in MPa;  $d$  – depth of compaction in m;  $S_{CP}$  – mean area of the cross section of the compacted material in  $m^2$ .

If the accepted slope angle of the compacted material (**Fig. 1**) is:  $2 \cdot 30 = 60$  degrees, the mean area of the cross section of the compacted material is calculated using the following equation

$$S_{CP} = \frac{L_{BAR}d}{2 \cos 30}, \quad (8)$$

where  $L_{BAR}$  – the length of the steel drum (width of compaction) in m.

After substitution of equation (8) in equation (7), the equation for the calculation of approximate value of stiffness coefficient for compacted material  $c_3$  in N/m is obtained

$$c_3 = \frac{E_M L_{BAR}}{2 \cos 30}. \quad (9)$$

### 3. Results and discussion

#### 3. 1. Developed overall mathematical model of the system "vibratory roller – compacted material"

The developed overall mathematical model of the "vibratory roller – compacted material" system (**Fig. 1**) with three degrees of freedom by which the dynamic behavior of the roller and front steel drum (i.e. compaction amplitude) can be obtained is shown in **Fig. 2**.

The following denotations are used in **Fig. 2**:

$x_1(t)$  and  $x_2(t)$  – the vertical displacements of the chassis suspension points at both ends of the roller – to the front steel drum and to the rear pneumatic tires

$x_3(t)$  – vertical displacement of the front steel drum;

$\theta(t)$  – rotation angle of the steel chassis;  
 $x(t)$  – vertical displacement of center of gravity of the roller chassis;  
 $H$  – vertical distance between the center of gravity and the horizontal plane of the suspension points of the roller chassis in m;  
 C.G. – center of gravity of steel chassis;  
 $L$  – horizontal distance between the front drum suspension point and the rear tires suspension point (equal to the wheelbase of the roller) in m;  
 $L_1$  – horizontal distance between the rear tire suspension point and the center of gravity in m;  
 $L_2$  – horizontal distance between the front drum suspension point and the center of gravity in m;  
 $m$  – own mass of the steel chassis of the roller (without the mass of the steel drum) in kg;  
 $J$  – mass moment of inertia of the chassis of the roller in  $\text{kg}\cdot\text{m}^2$ ;  
 $m_3$  – own mass of the steel roller drum (including unbalanced rotating parts) in kg;  
 $c_1$  – stiffness coefficient between the steel chassis of the roller and the compacted material at the rear end of the roller in N/m – **Fig. 2** (i.e.  $c_1$  includes the stiffness of the rear pneumatic tires plus the stiffness of the compacted material for the assumed depth of compaction  $d$  in m);  
 $c_2$  – stiffness coefficient between the steel chassis of the roller and the front steel drum at the front end of the roller in N/m – **Fig. 2** (i.e.  $c_2$  represents the stiffness of the vibration insulators, which are installed between the front drum and roller chassis);  
 $c_3$  – stiffness coefficient of the compacted material in N/m (for the assumed compaction depth  $d$  in m).

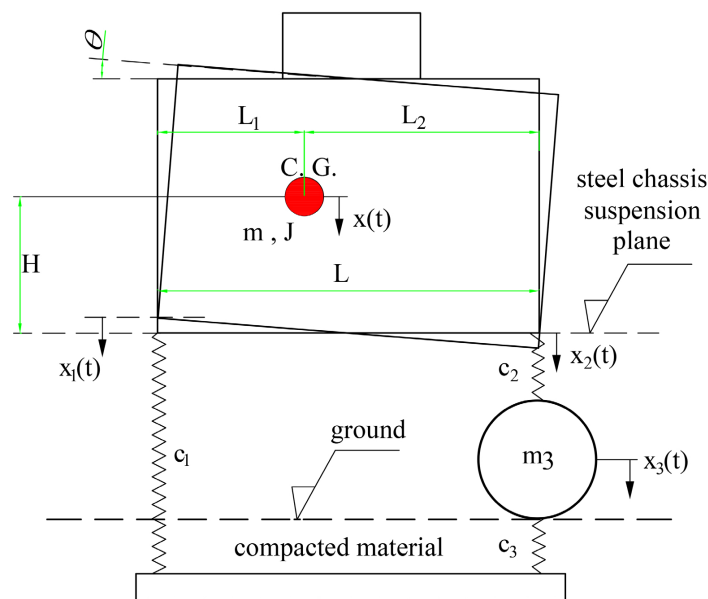


**Fig. 2.** Overall mathematical model by which the dynamic behavior of the roller is represented with three degrees of freedom –  $x_1(t)$ ,  $x_2(t)$  and  $x_3(t)$

The stiffness coefficient  $c_1$  can be calculated by the simplified equation in N/m

$$c_1 = c_3 \cdot c_T / (c_3 + c_T),$$

where  $c_T$  – the stiffness of the rear pneumatic tires in N/m.

The proposed overall model (**Fig. 2**) facilitates the consideration of multiple technical parameters influencing compaction performance, including material density, elastic modulus, excitation frequency, roller weight, and the position of the center of mass. Furthermore, it establishes a methodology for calculating the roller's compaction amplitude, developed with a focus on technological applicability. The lack of such a methodology for this purpose has been identified as a gap in the existing body of research.

For the present reviewed case (**Fig. 2**):  $Q_{x1}(t) = 0$ ;  $Q_{x2}(t) = 0$ ;  $Q_{x3}(t) = F_{DEB}(t)$ . The kinetic energy and the potential energy of the dynamic system, expressed by the generalized coordinates  $x(t)$ ,  $\theta(t)$  and  $x_3(t)$  are as follows:

$$E_K = \frac{m\dot{x}^2 + (J + mH^2)\dot{\theta}^2 + m_3\dot{x}_3^2}{2}, \quad (10)$$

$$E_P = \frac{c_1x^2 - 2c_1x\theta L_1 + c_1L_1^2\theta^2 + c_2x^2 + c_2x_3^2 + c_2L_2^2\theta^2 + 2c_2L_2\theta x - 2c_2L_2\theta x_3 - 2c_2x_3x + c_3x_3^2}{2}. \quad (11)$$

In **Fig. 2** it can be seen that the geometrical relationship of the generalized coordinates  $x(t)$ ,  $\theta(t)$  and the generalized coordinates  $x_1(t)$ ,  $x_2(t)$  is as follows:

$$\theta(t) = \frac{x_2(t) - x_1(t)}{L_1 + L_2} = \frac{x_2(t) - x_1(t)}{L}, \quad (12)$$

$$x(t) = \frac{L_2}{L}x_1(t) + \frac{L_1}{L}x_2(t). \quad (13)$$

After substituting of equations (12), (13) in equations (10), (11) and after performing elemental transformations, the kinetic energy and the potential energy of the dynamic system are obtained, expressed by the generalized coordinates  $x_1(t)$ ,  $x_2(t)$  and  $x_3(t)$ :

$$E_K = \frac{m\dot{x}_1^2L_2^2 + 2m\dot{x}_1L_2\dot{x}_2L_1 + m\dot{x}_2^2L_1^2 + (J + mH^2)(\dot{x}_1^2 + \dot{x}_2^2) - 2\dot{x}_2\dot{x}_1(J + mH^2) + m_3\dot{x}_3^2L^2}{2L^2}, \quad (14)$$

$$E_P = \frac{c_2x_2^2 + c_1x_1^2 - 2c_2x_2x_3 + c_2x_3^2 + c_3x_3^2}{2}. \quad (15)$$

After substitution of equations (2), (14), (15) in equations (3)–(5) and performing elemental transformations, the final three differential equations of dynamic motion are obtained, represented by the generalized coordinates  $x_1(t)$ ,  $x_2(t)$  and  $x_3(t)$  with included damping coefficients  $b$  in N·s/m:

$$\frac{(J + mH^2 + mL_2^2)}{L^2}\ddot{x}_1 - \frac{(J + mH^2 - mL_1L_2)}{L^2}\ddot{x}_2 + b_1\dot{x}_1 + c_1x_1 = 0, \quad (16)$$

$$\frac{(J + mH^2 + mL_1^2)}{L^2}\ddot{x}_2 - \frac{(J + mH^2 - mL_1L_2)}{L^2}\ddot{x}_1 + b_2\dot{x}_2 - b_2\dot{x}_3 + c_2x_2 - c_2x_3 = 0, \quad (17)$$

$$m_3\ddot{x}_3 - b_2\dot{x}_2 + (b_2 + b_3)\dot{x}_3 - c_2x_2 + (c_2 + c_3)x_3 = 2m_1e_1\omega_1^2 \sin(\omega_1 t), \quad (18)$$

where  $b_1$  – damping coefficient of rear pneumatic tires plus the compacted material in N·s/m (for the accepted depth of compaction  $d$  in m);  $b_2$  – damping coefficient of the vibration insulators, which are installed between the front drum and roller chassis (**Fig. 1**) in N·s/m;  $b_3$  – damping coefficient of the compacted material in N·s/m (for the accepted depth of compaction  $d$  in m).

### 3. 2. Accepted model input data

For the purposes of the present study, an exemplary model of a 10-tonne single-drum vibratory roller was analyzed, which has the following technical parameters:  $L = 3.1$  m,  $L_1 = 1.6$  m,  $L_2 = 1.5$  m,  $H = 0.6$  m,  $L_{BAR} = 1.8$  m,  $m = 6000$  kg,  $J = 6500$  kg·m<sup>2</sup>,  $m_3 = 3600$  kg,  $c_2 = 3200$  kN/m,  $b_2 = 125.43$  kN·s/m,  $c_T = 700$  kN/m,  $e_1 = 0.12$  m and  $m_1 = 25$  kg.

Three different values of exciting vibrational frequencies inside the front steel drum are analyzed:  $\omega_{1.1} = 157$  rad/sec ( $f_{1.1} = 25$  Hz);  $\omega_{1.2} = 282.6$  rad/sec ( $f_{1.2} = 45$  Hz);  $\omega_{1.3} = 471$  rad/sec ( $f_{1.3} = 75$  Hz).

The accepted input data for the mechanical characteristics of the five different types of analyzed compacted material are given in **Table 1**.

**Table 1**

Accepted model input data of the mechanical characteristics for the five different types of compacted material [23, 24]

No.	Types of compacted material	Accepted depth of compaction $d$ in m	Compressive strength of compacted material $\sigma$ in MPa (ground loading is assumed)	Module of elasticity of compacted material $E_M$ in MPa
1	Sand (particle size up to 0.5 cm) with density: $\gamma = 2.1 \text{ t/m}^3$	1.0	0.45	110
2	Gravel (particles size up to 3.0 cm) with density: $\gamma = 2.2 \text{ t/m}^3$	1.0	0.5	120
3	Crushed stone (particles size up to 10.0 cm) with density: $\gamma = 2.3 \text{ t/m}^3$	1.5	0.6	150
4	Cohesive clay soil with density: $\gamma = 1.8 \text{ t/m}^3$	0.5	0.25	50
5	Mixed soil/sand and clay/with density: $\gamma = 1.9 \text{ t/m}^3$	0.7	0.3	65

The calculated stiffness coefficients and damping coefficients are shown in **Table 2**.

**Table 2**

Calculated stiffness coefficients  $c$  [N/m] and damping coefficients  $b$  [N·s/m] for the different types of compacted material

No.	Types of compacted material	$c_3$ in N/m	$b_3$ in N·s/m	$c_1$ in N/m	$b_1$ in N·s/m
1	Sand (particle size up to 0.5 cm) with density: $\gamma = 2.1 \text{ t/m}^3$	114 318 707	1 399 970	466 663	58 890
2	Gravel (particles size up to 3.0 cm) with density: $\gamma = 2.2 \text{ t/m}^3$	124 711 200	1 462 220	473 381	59 313
3	Crushed stone (particles size up to 10.0 cm) with density: $\gamma = 2.3 \text{ t/m}^3$	155 889 000	1 634 812	490 133	60 353
4	Cohesive clay soil with density: $\gamma = 1.8 \text{ t/m}^3$	51 963 000	943 859	401 921	54 653
5	Mixed soil/sand and clay/with density: $\gamma = 1.9 \text{ t/m}^3$	67 551 900	1 076 165	424 125	56 142

### 3.3. Obtained results by solving the differential equations of dynamic motion

After solving the three differential equations of dynamic motion (16)–(18) for the first type of compacted material (sand, particle size up to 0.5 cm, density:  $\gamma = 2.1 \text{ t/m}^3$ ) and with the first analyzed value of input excitation frequency ( $\omega_{1,1} = 157 \text{ rad/sec}$ ,  $f_{1,1} = 25 \text{ Hz}$ ) the following results were obtained, which are presented in **Fig. 3**.

The results presented in **Fig. 3** indicate that the dynamic system operates in a steady-state vibration regime without any increasing amplitudes (**Fig. 3, a–c**). The vibration insulators demonstrated high performance, as the vibration amplitude transmitted to the steel chassis,  $x_2(t)$  (**Fig. 3, b**) was approximately three times lower than the vibration amplitude measured at the steel drum,  $x_3(t)$  (**Fig. 3, c**).

The three differential equations of dynamic motion (16)–(18) are solved in the same manner for the other analyzed cases (different types of compacted soil and different input excitation frequencies) and the obtained results are summarized and given in **Table 3**.

The results presented in **Table 3** show that the highest compaction amplitude, among the three analyzed frequencies, was achieved at the maximum input excitation frequency of:  $f = 75 \text{ Hz}$  (**Table 3**). However, this comparison across different excitation frequencies (i.e. 25 Hz, 45 Hz, and 75 Hz) should not be considered fully reliable in practical applications, as the elasticity of the steel components of the roller chassis and steel drum was neglected in the analyzed model, since this simplification may significantly affect the predicted compaction amplitude at higher excitation frequencies.

The highest compaction amplitudes, among the five analyzed types of compacted materials, are logically observed in combinations involving cohesive clay soils and mixed clay soils,

because of the lower clay stiffness. However, it is well-known, that the use of a vibratory roller for compacting clay soils is not recommended in practice, as vibration waves propagation through clay are highly attenuated. When considering only the compaction amplitudes of non-cohesive materials (e.g., stones, gravel, sand), the results indicate that the greatest compaction efficiency (expressed through compaction amplitude) for the exemplary vibratory roller model is expected when compacting sands (i.e. non-cohesive granular soils) with small particle sizes up to 0.5 cm.

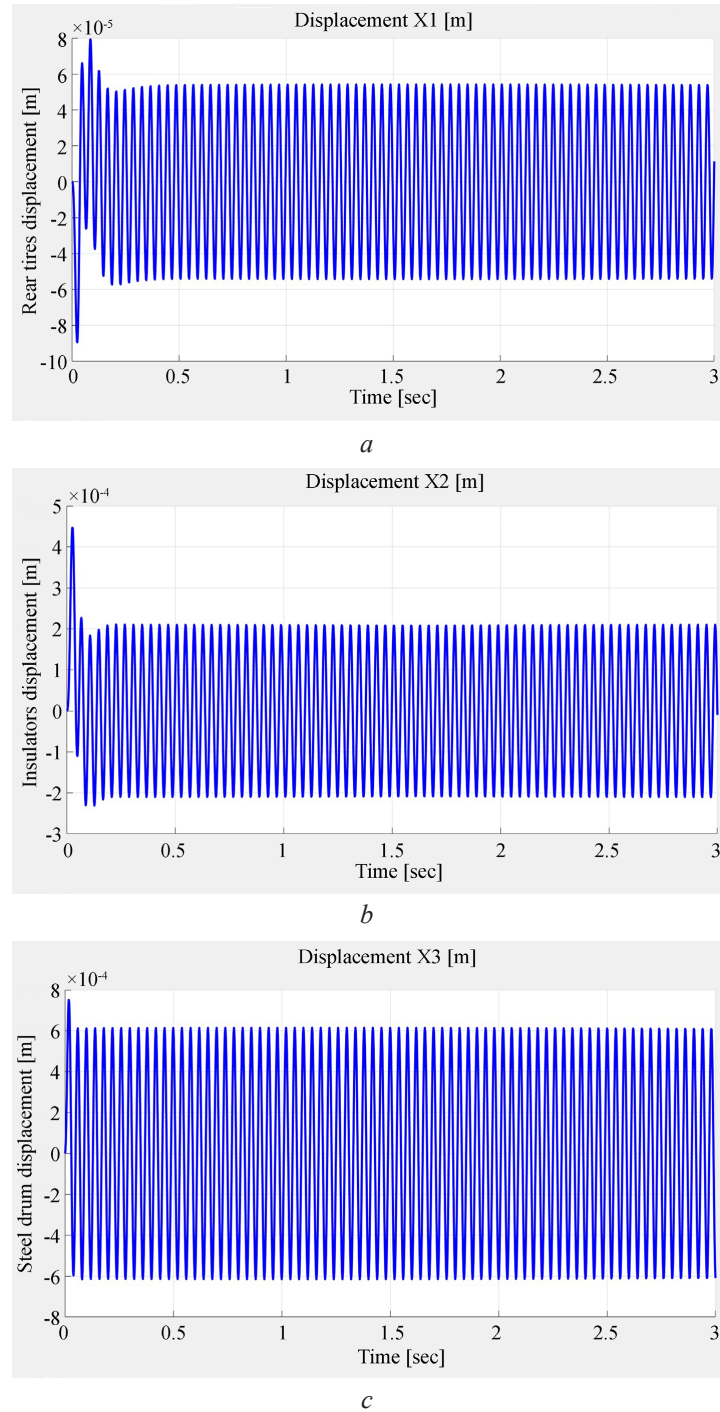


**Fig. 3.** Obtained results for the first type of compacted material (sand, particle size up to 0.5 cm, density:  $\gamma = 2.1 \text{ t/m}^3$ , excitation frequency:  $f_{1.1} = 25 \text{ Hz}$ ): *a* – vertical displacement of roller steel chassis at the rear pneumatic tires,  $x_1(t)$ ; *b* – vertical displacements of roller chassis to the front steel drum (at the vibration insulators),  $x_2(t)$ ; *c* – vertical displacement of the front steel drum,  $x_3(t)$

**Table 3**

Obtained results for maximum vertical displacement (amplitude) of the front steel drum  $x_3$  in m (i.e. amplitude of compaction) for the different types of compacted soil and the different input excitation frequencies

Types of compacted material	Analyzed values of the input excitation frequencies (i.e. rotational speeds of unbalanced rotating shafts inside the vibratory drum): $\omega_1$ in rad/sec		
	$\omega_{1,1} = 157$ rad/sec ( $f_{1,1} = 25$ Hz)	$\omega_{1,2} = 282.6$ rad/sec ( $f_{1,2} = 45$ Hz)	$\omega_{1,3} = 471$ rad/sec ( $f_{1,3} = 75$ Hz)
Sand (particle size up to 0.5 cm) with density: $\gamma = 2.1$ t/m <sup>3</sup>	$x_1 = 54.10^{-6}$ m	$x_1 = 50.10^{-6}$ m	$x_1 = 39.10^{-6}$ m
	$x_2 = 208.10^{-6}$ m	$x_2 = 195.10^{-6}$ m	$x_2 = 150.10^{-6}$ m
	$x_3 = 615.10^{-6}$ m	$x_3 = 1028.10^{-6}$ m	$x_3 = 1321.10^{-6}$ m
Gravel (particles size up to 3.0 cm) with density: $\gamma = 2.2$ t/m <sup>3</sup>	$x_1 = 52.10^{-6}$ m	$x_1 = 49.10^{-6}$ m	$x_1 = 38.10^{-6}$ m
	$x_2 = 201.10^{-6}$ m	$x_2 = 189.10^{-6}$ m	$x_2 = 149.10^{-6}$ m
	$x_3 = 589.10^{-6}$ m	$x_3 = 1002.10^{-6}$ m	$x_3 = 1313.10^{-6}$ m
Crushed stone (particles size up to 10.0 cm) with density: $\gamma = 2.3$ t/m <sup>3</sup>	$x_1 = 45.10^{-6}$ m	$x_1 = 46.10^{-6}$ m	$x_1 = 37.10^{-6}$ m
	$x_2 = 179.10^{-6}$ m	$x_2 = 189.10^{-6}$ m	$x_2 = 144.10^{-6}$ m
	$x_3 = 518.10^{-6}$ m	$x_3 = 930.10^{-6}$ m	$x_3 = 1265.10^{-6}$ m
Cohesive clay soil with density: $\gamma = 1.8$ t/m <sup>3</sup>	$x_1 = 76.10^{-6}$ m	$x_1 = 61.10^{-6}$ m	$x_1 = 43.10^{-6}$ m
	$x_2 = 292.10^{-6}$ m	$x_2 = 236.10^{-6}$ m	$x_2 = 167.10^{-6}$ m
	$x_3 = 857.10^{-6}$ m	$x_3 = 1243.10^{-6}$ m	$x_3 = 1473.10^{-6}$ m
Mixed soil /sand and clay/with density: $\gamma = 1.9$ t/m <sup>3</sup>	$x_1 = 68.10^{-6}$ m	$x_1 = 58.10^{-6}$ m	$x_1 = 42.10^{-6}$ m
	$x_2 = 266.10^{-6}$ m	$x_2 = 224.10^{-6}$ m	$x_2 = 163.10^{-6}$ m
	$x_3 = 776.10^{-6}$ m	$x_3 = 1179.10^{-6}$ m	$x_3 = 1435.10^{-6}$ m

The results presented in **Table 3** indicate that at a low excitation frequency of 25 Hz, the ratio between the compaction amplitudes of granular soils with small particles (up to 0.5 cm) and granular soils with large particles (up to 10 cm) is  $0.615 \text{ mm}/0.518 \text{ mm} = 1.19$  (**Table 3**). In other words, the compaction amplitude (consequently the compaction efficiency) of granular soils with small particles is 1.19 times higher than that of granular soils with large particles for the exemplary vibratory roller model. At a higher excitation frequency of 75 Hz, this ratio decreases significantly  $1.321 \text{ mm}/1.265 \text{ mm} = 1.04$  to (**Table 3**). This finding suggests that, for the exemplary single-drum vibratory roller model, at 25 Hz, the influence of particle size on compaction amplitude is significant, with ratio of about 1.19 times. Conversely, at 75 Hz, the influence of particle size on compaction amplitude becomes minimal, with a ratio of only 1.04.

For practical applications recommend the compaction amplitude of a given single-drum vibratory roller model be evaluated through a comprehensive dynamic analysis of multi-degree-of-freedom systems, using the real technical specifications of the roller (e.g., own mass, excitation frequency) and the actual mechanical properties of the compacted material (e.g., density, elastic modulus). Since the elasticity of the steel components of the roller chassis and steel drum was neglected in the present analysis (an assumption that can substantially influence the compaction amplitude at high excitation frequencies) comparisons of compaction amplitudes obtained at different excitation frequencies (e.g., 25 Hz and 75 Hz) should not be considered fully reliable and applicable in practice. Therefore, the proposed methodology is recommended for use under a fixed available excitation frequency of a single-drum vibratory roller (e.g., 25 Hz) to compare the calculated compaction amplitudes when compacting different types of non-cohesive granular soils (such as sand, gravel, or crushed stone), in order to determine the most suitable roller – material combination and thereby enhance compaction efficiency and productivity at the building site.

Future researches by the authors will focus on developing more comprehensive mathematical models of the "vibratory roller – compacted material" system which incorporate the stiffness of the roller's steel chassis and steel drum, as well as a potential non-linear behavior (i.e. variable stiffness) of the upper layer of the compacted material.

#### 4. Conclusions

1. It is developed an analytical methodology, which is aimed at improving the efficiency of compaction operations using single-drum vibratory rollers. The methodology is based on a newly formulated overall mathematical model with three degrees of freedom representing the "vibratory roller – compacted material" system, through which the vibration amplitude of the roller's steel drum can be determined.

2. The presented methodology adopts a technological approach for identifying the most appropriate combination between the technical parameters of a single-drum vibratory roller and the mechanical characteristics of the compacted material, which enables consideration of multiple influencing parameters, including: elasticity modulus, material density, excitation frequency, center of mass position and roller weight.

3. It is provided an illustrative example, which demonstrates the application of the proposed methodology, using an exemplary single-drum vibratory roller model with three possible excitation frequencies and five different types of compacted materials.

#### Conflict of interest

The authors declare that they have no conflict of interest in relation to this study, whether financial, personal, authorship or otherwise, that could affect the study and its results presented in this paper.

#### Financing

The study was performed without financial support.

#### Data availability

Data will be made available on reasonable request.

#### Use of artificial intelligence

The authors confirm that they did not use artificial intelligence technologies when creating the current work.

#### Acknowledgement

The authors would like to thank the University of Architecture, Civil Engineering and Geodesy – Sofia for giving them the conditions to conduct this study.

#### Authors' contributions

**Kalin Radlov:** Investigation, Methodology, Writing – review & editing.

**Latchezar Lazov:** Formal analysis, Software, Validation.

**Andrey Totsev:** Conceptualization, Data curation, Supervision.

**Latchezar Hristchev:** Visualization, Writing – original draft.

---

#### References

- [1] Korchagin, P. A., Teterina, I. A., Korchagina, E. A. (2021). Road roller operator's vibroprotection system improvement. *Journal of Physics: Conference Series*, 1791 (1), 012012. <https://doi.org/10.1088/1742-6596/1791/1/012012>
- [2] Nguyen, V., Zhang, J., Le, V., Jiao, R. (2018). Vibration Analysis and Modeling of an Off-Road Vibratory Roller Equipped with Three Different Cab's Isolation Mounts. *Shock and Vibration*, 2018 (1). <https://doi.org/10.1155/2018/8527574>
- [3] Duy, N. T., Van Quynh, L., Ha, D. V., Van Cuong, B., Long, L. X. (2021). Ride comfort evaluation for a double-drum vibratory roller with semi-active hydraulic cab mount system. *E3S Web of Conferences*, 304, 01008. <https://doi.org/10.1051/e3sconf/202130401008>
- [4] Kadivar, H. T. (2016). Case study on output/productivity of pneumatic tired vibratory roller (earth compaction equipment) under different job and management conditions. *IJSTE – International Journal of Science Technology and Engineering*, 3 (04). Available at: [https://www.academia.edu/30825942/Case\\_Study\\_on\\_Output\\_Productivity\\_of\\_Pneumatic\\_Tired\\_Vibratory\\_Roller\\_Earth\\_Compaction\\_Equipment\\_under\\_Different\\_Job\\_and\\_Management\\_Conditions](https://www.academia.edu/30825942/Case_Study_on_Output_Productivity_of_Pneumatic_Tired_Vibratory_Roller_Earth_Compaction_Equipment_under_Different_Job_and_Management_Conditions)
- [5] Kurdyumov, V. I., Proshkin, V. E., Zykin, E. S., Proshkin, E. N., Kurushin, V. V. (2022). Studies of the vibratory roller from the standpoint of compliance with the agrotechnical requirements of soil density and structure. *IOP Conference Series: Earth and Environmental Science*, 1045 (1), 012030. <https://doi.org/10.1088/1755-1315/1045/1/012030>

- [6] Rakhimov, I. R., Telichkina, N. A., Batraeva, O. S., Shabunin, A. A., Krasnozhon, S. M. (2019). Substantiating the Parameters of a Two-drum Roller for Tillage. IOP Conference Series: Materials Science and Engineering, 582 (1), 012027. <https://doi.org/10.1088/1757-899x/582/1/012027>
- [7] Mohamed, A. (2005). Load calculation and simulation of an asphalt roller. Karlskrona. Available at: <https://www.diva-portal.org/smash/get/diva2:831499/FULLTEXT01.pdf>
- [8] Nilov, V., Zhulai, V., Tyunin, V., Schienko, A. (2022). Substantiation of the necessity of creating three-drum road rollers. Transportation Research Procedia, 63, 2767–2772. <https://doi.org/10.1016/j.trpro.2022.06.320>
- [9] Zhang, Q., An, Z., Huangfu, Z., Li, Q. (2022). A Review on Roller Compaction Quality Control and Assurance Methods for Earthwork in Five Application Scenarios. Materials, 15 (7), 2610. <https://doi.org/10.3390/ma15072610>
- [10] Fujita, H., Tsukimoto, Y. (2017). Successful compaction using vibratory pneumatic tire roller. 17-th AAPA International Flexible Pavements Conference 2017. Available at: [https://www.sakainet.co.jp/en/technology/item/successful\\_compaction\\_using\\_vibratory\\_pneumatic\\_tire\\_roller.pdf](https://www.sakainet.co.jp/en/technology/item/successful_compaction_using_vibratory_pneumatic_tire_roller.pdf)
- [11] Tarasov, V. N., Boyarkina, I. V., Serebrennikov, V. S. (2019). Analytical study of oscillating horizontal vibrations of a road roller. Journal of Physics: Conference Series, 1260 (11), 112027. <https://doi.org/10.1088/1742-6596/1260/11/112027>
- [12] Abd El Halim, A. E. H. O., Mostafa, A. (2006). Asphalt Multi-Integrated Rollers and Steel Drum Compactors. Transportation Research Record: Journal of the Transportation Research Board, 1967 (1), 173–180. <https://doi.org/10.1177/0361198106196700117>
- [13] Bian, Y., Yang, M., Fang, X., Wang, X. (2017). Kinematics and Path Following Control of an Articulated Drum Roller. Chinese Journal of Mechanical Engineering, 30 (4), 888–899. <https://doi.org/10.1007/s10033-017-0102-8>
- [14] White, D., Vennapusa, P. K. R. (2010). A review of roller-integrated compaction monitoring technologies for earthworks. Final Report No: ER10-04. Earthworks Engineering Research Center (EERC). Available at: [https://www.intrans.iastate.edu/wp-content/uploads/2018/03/White-and-Vennapusa-2010\\_FHWA-IC-Lit-Review.pdf](https://www.intrans.iastate.edu/wp-content/uploads/2018/03/White-and-Vennapusa-2010_FHWA-IC-Lit-Review.pdf)
- [15] Qin, G., Zou, Q., Li, M., Deng, Y., Mi, P., Zhu, Y., Liu, H. (2025). Surface defect detection on industrial drum rollers: Using enhanced YOLOv8n and structured light for accurate inspection. PLOS ONE, 20 (2), e0316569. <https://doi.org/10.1371/journal.pone.0316569>
- [16] Wersall, C. (2016). Frequency optimization of vibratory rollers and plates for compaction of granular soil. Doctoral Thesis, Department of Civil and Architectural Engineering. Stockholm. Available at: <https://www.diva-portal.org/smash/get/diva2:929931/FULLTEXT01.pdf>
- [17] Pistor, J., Hager, M., Kopf, F., Adam, D. (2023). Consideration of the Variable Contact Geometry in Vibratory Roller Compaction. Infrastructures, 8 (7), 110. <https://doi.org/10.3390/infrastructures8070110>
- [18] Liu, L., Wang, F., Sun, S., Feng, W., Guo, C. (2021). Nonlinear Dynamics of the Rigid Drum for Vibratory Roller on Elastic Subgrades. Shock and Vibration, 2021 (1). <https://doi.org/10.1155/2021/9589230>
- [19] Capatina, D., Nitu, M. Cr., Iliescu, M. (2023). Modelling the vibratory roller compaction process of road soils, Archives of Civil Engineering Journal, LXIX (4), 431–444. <https://doi.org/10.24425/ace.2023.147668>
- [20] Li, S., Hu, C. (2018). Study on Dynamic Model of Vibratory Roller – Soil System. IOP Conference Series: Earth and Environmental Science, 113, 012187. <https://doi.org/10.1088/1755-1315/113/1/012187>
- [21] EN 1991-3 (2006) (English): Eurocode 1: Actions on structures – Part 3: Actions induced by cranes and machinery [Authority: The European Union Per Regulation 305/2011, Directive 98/34/EC, Directive 2004/18/EC]. Available at: <https://www.phd.eng.br/wp-content/uploads/2015/12/en.1991.3.2006.pdf>
- [22] De Silva, C. (1999). Vibration – Fundamentals and Practice. CRC Press, 939. Available at: [https://www.academia.edu/49116020/By\\_Clarence\\_W\\_de\\_Silva](https://www.academia.edu/49116020/By_Clarence_W_de_Silva)
- [23] Ilov, G. (2012). Rakovodstvo po Geotehnika. razraboteno saglasno iziskvaniqta na Evrokod 7 – Geotehnichesko proektirane. Sofia, 456.
- [24] Ilov, G., Totzev, A. (2023). Klasicheska Geotehnika. Vol. I. Sofia, 290. Available at: <https://eclipse.uacg.bg/catalog/view/QEY8CYLEDW>

Received 06.08.2025

Received in revised form 10.09.2025

Accepted 13.11.2025

Published 28.11.2025

© The Author(s) 2025

This is an open access article  
under the Creative Commons CC BY license  
<https://creativecommons.org/licenses/by/4.0/>

**How to cite:** Radlov, K., Lazov, L., Totzev, A., Hristchev, L. (2025). Developing a methodology for improving the efficiency of the compaction of a base course with a single-drum vibratory roller. EUREKA: Physics and Engineering, 6, 97–107. <http://doi.org/10.21303/2461-4262.2025.003925>